

## **CAPÍTULO IV**

**The Anicuns Volcano-Sedimentary Sequence at the limit between the juvenile Goiás Magmatic Arc and the western edge of the São Francisco Continent: new geochemical and Nd isotopic data of metabasic and metasedimentary rocks**

Jorge Henrique Laux  
Márcio Martins Pimentel  
Simone M. C. L. Gioia

## 4.1 INTRODUCTION

The Goiás Magmatic Arc, in central Brazil, consists of several arc-type metavolcano-sedimentary sequences associated with tonalitic to granitic orthogneisses, forming an extensive Neoproterozoic juvenile terrain along the western part of the Brasília Belt (Pimentel and Fuck, 1992; Pimentel et al., 2000a). Mafic volcanic and plutonic rocks are associated with calc-alkaline andesites, dacites, and rhyolites in some of these sequences (e.g. Bom Jardim de Goiás and Arenópolis; Seer, 1985; Pimentel and Fuck, 1986), but they also form bimodal associations with rhyolites in others (e.g. Iporá and Jaupaci sequences) (Pimentel et al., 1991; Rodrigues et al., 1999). The metavolcanic rocks typically present very primitive geochemical and isotopic characteristics, with low initial  $^{87}\text{Sr}/^{86}\text{Sr}$  ratios and positive  $\varepsilon_{\text{Nd}}(\text{T})$  values. Felsic metavolcanic rocks have U-Pb zircon ages between ca. 0.9 and 0.64 Ga (Pimentel et al., 1991; Rodrigues et al., 1999). Most of the previous isotopic, geochronological and petrological studies concentrated on intermediate to felsic members of this magmatism, and little is known about the associated mafic rocks. Fine-grained amphibolites of the Arenópolis volcano-sedimentary sequence are probably the best-known representatives of these Neoproterozoic mafic metavolcanic rocks. They comprise low-K tholeiites to calc-alkaline metabasalts, with primitive isotopic compositions (initial  $^{87}\text{Sr}/^{86}\text{Sr}$  of ca. 0.7026 and  $\varepsilon_{\text{Nd}}(\text{T})$  of ca. +6.9; Pimentel, 1991), representing the early stages of development of an intraoceanic island arc system. Small metamorphosed gabbro-diorite intrusions are also recognized within the Arenópolis Sequence, and one has been recently dated at  $890 \pm 9$  Ma (SHRIMP U-Pb zircon age; Pimentel et al., 2003), corresponding to plutonic/subvolcanic equivalent of the volcanic sequence.

The Anicuns-Itaberaí Sequence, exposed along the contact between the eastern part of the Goiás Magmatic Arc and the Anápolis-Itauçu high-grade terrain, is represented dominantly by amphibolites (metavolcanic and metaplutonic) and

metapelitic rocks, with subordinate iron formation, chert, marble, and ultramafic rocks of uncertain age. It has been correlated, in the past, with the Archean Serra de Santa Rita greenstone belt, exposed to the north (Barbosa, 1987), or with Paleoproterozoic sequences such as the Silvânia Sequence to the west of Anápolis-Itaçu Complex (Lacerda Filho et al., 1991) and the Mossâmedes volcanics (Nunes, 1990). Recent studies based mainly on Sm-Nd isotopic characteristics of the Anicuns-Itaberaí rocks, however, suggest that they are considerably younger and might be part of the Neoproterozoic Goiás Magmatic Arc (Pimentel et al., 2000a, b; Laux et al., 2001, 2002a, b, 2004a).

In this paper we discuss new geochemical and isotopic data of coarse-grained mafic rocks exposed within the Anicuns-Itaberaí Sequence, which demonstrate that this rock assemblage belongs to the Goiás Magmatic Arc and might represent the boundary area between the juvenile arc and older sialic terrains belonging to the western edge of the Neoproterozoic São Francisco continent.

## **4.2 REGIONAL GEOLOGICAL SETTING**

The Tocantins Province represents a large Brasiliano/Pan-African orogen that developed between three major Neoproterozoic continents: the Amazon, São Francisco, and Paranapanema/Paraná. The province comprises three main fold belts, known as the Paraguay Belt in the southwest, the Araguaia Belt in the NW, and the Brasília Belt underlying large areas of the eastern part of the Tocantins Province, along the western margin of the São Francisco Craton (for a review see Pimentel et al., 2000a).

The Brasília Belt represents one of the best preserved and the most complete Neoproterozoic orogens in Brazil, comprising: (i) a thick Meso-Neoproterozoic sedimentary pile that includes the Paranoá, Canastra, Araxá, Ibiá, Vazante, and Bambuí groups, overlying mostly Paleoproterozoic and minor Archean basement (Almeida et al., 1981; Fuck et al., 1993, 1994, 2001; Pimentel et al., 2000a, b); (ii) the Goiás Massif, a micro-plate (or allochthonous sialic terrain) composed of Archean

rock units (the Crixás-Goiás granite-greenstones) and associated Proterozoic formations, and (iii) a large Neoproterozoic juvenile arc in the west (Goiás Magmatic Arc) (Fig. 4.1).

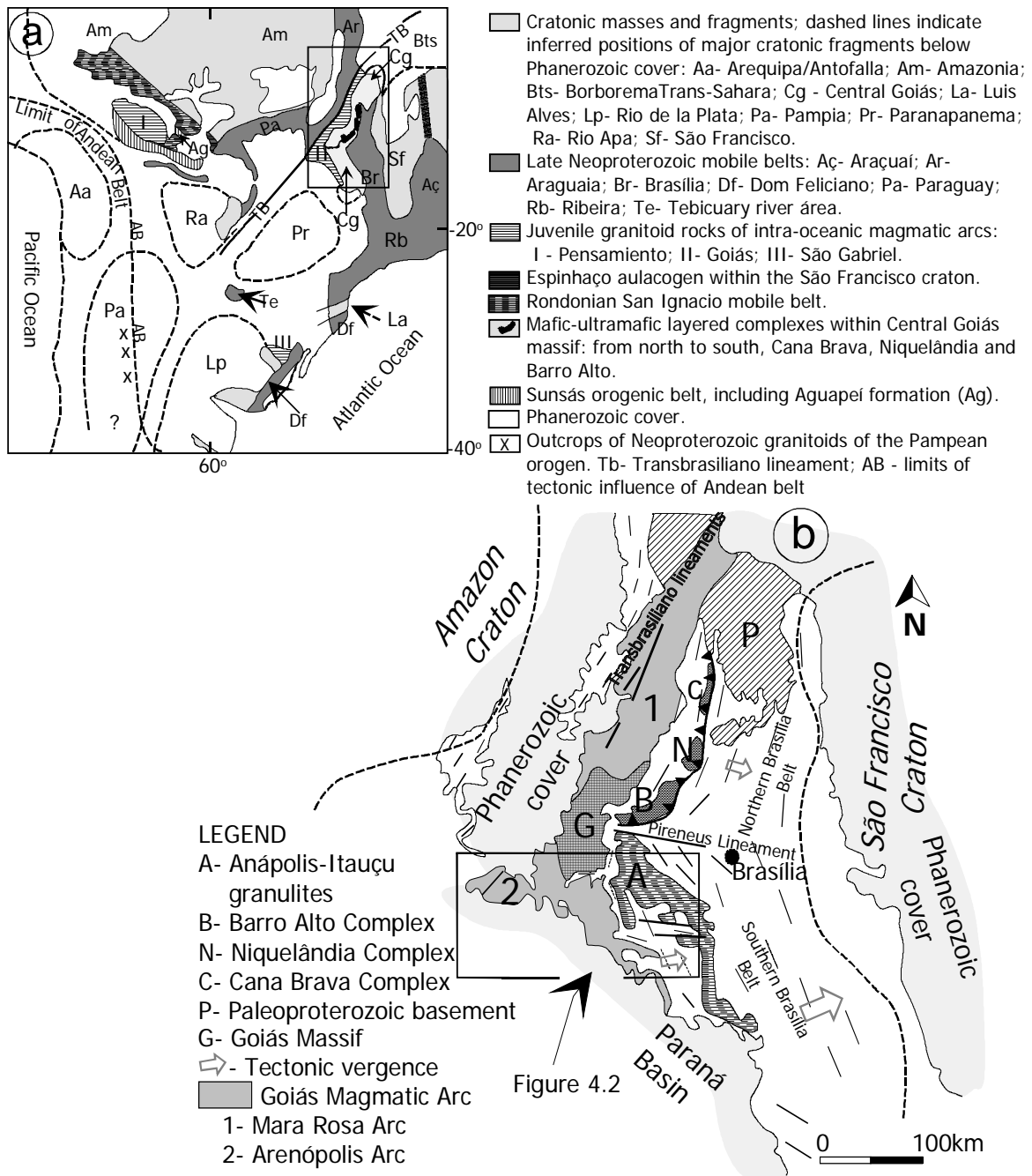


**Figure 4.1** – a) Precambrian tectonic framework of Central South America (after Kröner and Cordani, 2003; Cordani et al., 2003; b) Geological sketch map of the Brasília Belt in the eastern part of Tocantins Province, central Brazil (after Pimentel et al., 2003).

The several sedimentary/metasedimentary rock units, which occur in the eastern part of the Brasília Belt, display tectonic vergence to the east, towards the São Francisco Craton. They are more intensely deformed and metamorphosed

towards the west, reaching amphibolite facies conditions in the central part of the belt (Fuck et al., 1993, 1994; Dardenne, 2000).

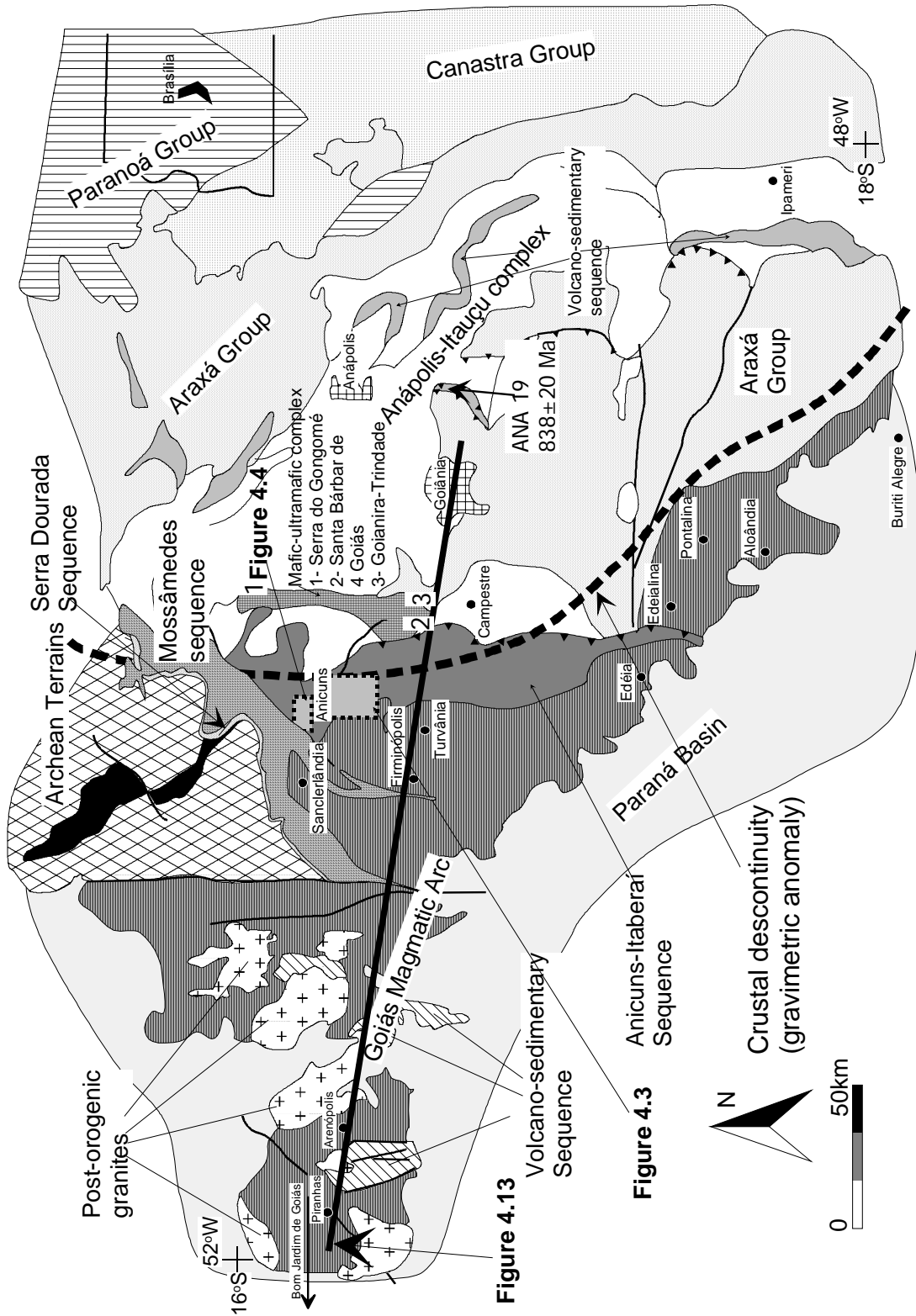


**Figure 4.2** - Geological sketch map of the southern part of the Goiás Magmatic Arc, with location of the areas investigated (after Pimentel et al., 2000a).

Metasedimentary rocks belonging to the Araxá and Canastra groups underlie

large areas in the central-southern part of the Brasília Belt (Figs. 4.1 and 4.2). Nappes and thrust sheets of these units overlie Paleoproterozoic basement represented by 2.1 Ga volcano-sedimentary sequences and associated granites (e.g. Silvânia and Rio do Peixe sequences and Jurubatuba granite; Fischel et al., 2001a, b; Piuzana et al., 2003a).

High-grade rocks of the Anápolis-Itauçu Complex are exposed in the central-southern part of the belt (Figs. 4.1 and 4.2). They include para- and orthogranulites, as well as strongly deformed intrusive granites. Recent data have indicated that the Nd isotopic signatures and metamorphic ages of the Araxá metasedimentary rocks, Anápolis-Itauçu felsic granulites, and intrusive granites are all very similar (Fischel et al., 1998, 1999; Pimentel et al., 1999, 2001; Seer, 1999; Piuzana et al. 2003a, b), demonstrating that at least part of the aluminous granulites of the Anápolis-Itauçu Complex may represent high-grade equivalents of the Araxá metasedimentary rocks. Therefore, source areas of the original Araxá sediments may have included Neoproterozoic juvenile areas such as the Goiás Magmatic Arc (Fischel et al., 1998, 1999; Pimentel et al., 1999, 2001; Piuzana et al., 2003a).

In the central part of the Brasília Belt is the Goiás Massif (Figs. 4.1 and 4.2), represented by: (i) Archean greenstone belts and TTG orthogneisses; (ii) Paleoproterozoic orthogneisses largely covered by younger supracrustal rocks; (iii) and mafic-ultramafic layered complexes of Barro Alto, Niquelândia, and Canabrava and associated volcano-sedimentary sequences. The eastern margin of the Goiás Massif is marked by a regional gravimetric discontinuity typical of suture zones (Haralyi and Hasui 1981; Marangoni et al., 1995). Therefore, the massif is interpreted as an allochthonous block amalgamated to the Brasília Belt during the Neoproterozoic (Brito Neves and Cordani, 1991; Pimentel et al., 2000b).

The Neoproterozoic juvenile arc (Goiás Magmatic Arc) is composed of volcano-sedimentary sequences associated with calcic to calc-alkaline tonalite/granodiorite gneisses (Fig. 4.2). The main arc terrenas are known as the Arenópolis and Mara Rosa arcs, located in western and northern Goiás, respectively (Pimentel and Fuck, 1992; Pimentel et al., 1991, 1997) (Fig. 4.1). In both areas, geological evolution started at ca. 890 - 860 Ma in intraoceanic island arcs with the crystallization of very

primitive tholeiitic to calc-alkaline volcanics and associated tonalites/granodiorites. These rocks have  $\epsilon_{\text{Nd}}(T)$  values between ca. +3.0 and +6.0 and  $T_{\text{DM}}$  values mostly between ca. 0.8 and 1.1 Ga (Pimentel et al., 1991, 1997, 2000b; Pimentel and Fuck, 1992). Geochemical and isotopic data (Pimentel, 1991; Pimentel et al., 1997) suggest that the original tonalitic/andesitic magmas were similar to modern adakites, commonly positioned above subduction zones where young and hot oceanic lithosphere was subducted under oceanic lithosphere. Calc-alkaline igneous activity was recurrent during the Neoproterozoic and lasted until ca. 640 Ma, with younger magmas becoming progressively more evolved. The main metamorphic episode occurred at ca. 630 Ma, as indicated by U-Pb titanite and Sm-Nd garnet ages (for a review, see Pimentel et al., 2000a), when final ocean closure probably took place.

There has been considerable debate on the real area distribution of these juvenile terrains, since geochronological and isotopic data are still sparse and insufficient. Recent U-Pb and Sm-Nd data have shown that the juvenile arc extends to the southeast and northeast, disappearing under the Paraná and Parnaíba Phanerozoic basins, respectively (Figs. 4.1 and 4.2). They underlie a very large area, which constitutes a significant portion of the Brasília Belt (Pimentel et al., 2000a; Fuck et al., 2001). In this context, the Anicuns-Itaberaí sequence represents a key geological unit for the understanding of the evolution of the Goiás Magmatic Arc and adjacent terrains because: (i) it represents one of the largest supracrustal sequences within this tectonic unit, (ii) it has been traditionally considered to be an Archean or Paleoproterozoic greenstone sequence, and (iii) it coincides with a regionally important gravimetric discontinuity, separating a gravimetric high to the west and a gravimetric low to the east (Baêta Junior, 1994).

#### **4.3 GEOLOGY OF THE ANICUNS REGION**

In the Mossâmedes-Anicuns region (Figs. 4.2, 4.3, and 4.4), Barbosa (1987) recognized three distinct supracrustal sequences and assigned different ages to them based on field relationships and structural data: (i) the Anicuns-Itaberaí Sequence

(AIS) was interpreted as the southern extension of the Serra de Santa Rita (Goiás Velho) greenstone belt, (ii) the Mossâmedes Sequence (Simões, 1984), west/northwest of Anicuns, was interpreted to be of Mesoproterozoic age, equivalent to the Araxá Group, and (iii) a younger detrital sequence (conglomerates, quartzites and schists) forming the roughly E-W Serra Dourada ridge to the north. The north/south supracrustal sequence, referred to as the Anicuns-Itaberaí Sequence (AIS) by Barbosa (1987), was divided into two distinct geological units by Nunes (1990): (i) the Córrego da Boa Esperança Sequence (CBES) in the west, correlated with the Araxá Group, consists of metapelites, andesitic/dacitic meta-tuffs, and iron formation (Nunes, 1990) (Fig. 4.3); (ii) the AIS in the east, separated from the CBES by a NNW reverse fault, is composed of mafic/ultramafic metavolcanic rocks, metacherts, metarhytmities, and marble lenses. Laux et al. (2004a) have demonstrated that the Anicuns-Itaberaí and Córrego da Boa Esperança sequences are of the same age and their supracrustal rocks formed between ca. 890 and 830 Ma and, therefore, belong to the Goiás Magmatic Arc.

Both Nunes (1990) and Barbosa (1987) have suggested that the metavolcanic rocks in this region have calc-alkaline or calc-alkaline/tholeiitic nature, indicating a magmatic arc setting for their origin. This was also suggested by Nilson (1981) for the country-rocks of the Americano do Brasil mafic-ultramafic layered complex exposed to the north of Anicuns.

Granitic rocks, as well as small mafic and mafic-ultramafic bodies are intrusive into the supracrustal sequences. The granitoid intrusions are tonalites, granodiorites, and granites with subordinate quartz syenite, monzonites, and monzodiorites (Barbosa, 1987; Nunes, 1990). The deformed, elongated, locally mylonitic granitic bodies, which represent the major part of the granite intrusive complexes in the area have been dated at approximately 800 Ma, whereas the late-tectonic, less voluminous granite intrusions are ca. 615 Ma old (Laux et al., 2004b).

Mafic/intermediate intrusions are collectively referred to as the Anicuns-Santa Bárbara Gabbro-Diorite Suite (Lacerda Filho and Oliveira, 1995). The Córrego Seco Complex (Fig. 4.3) comprises gabbro, diorite, amphibolite and, in some places, crosscutting relationships with the AIS are observed. This suite has been correlated

with the Americano do Brasil intrusion, exposed to the north of the AIS (Pfirner et al., 1981; Nunes, 1990). A diorite sample from this suite was dated at  $622 \pm 6$  Ma which has been interpreted as the crystallization age of the intrusion (Laux et al., 2004a).

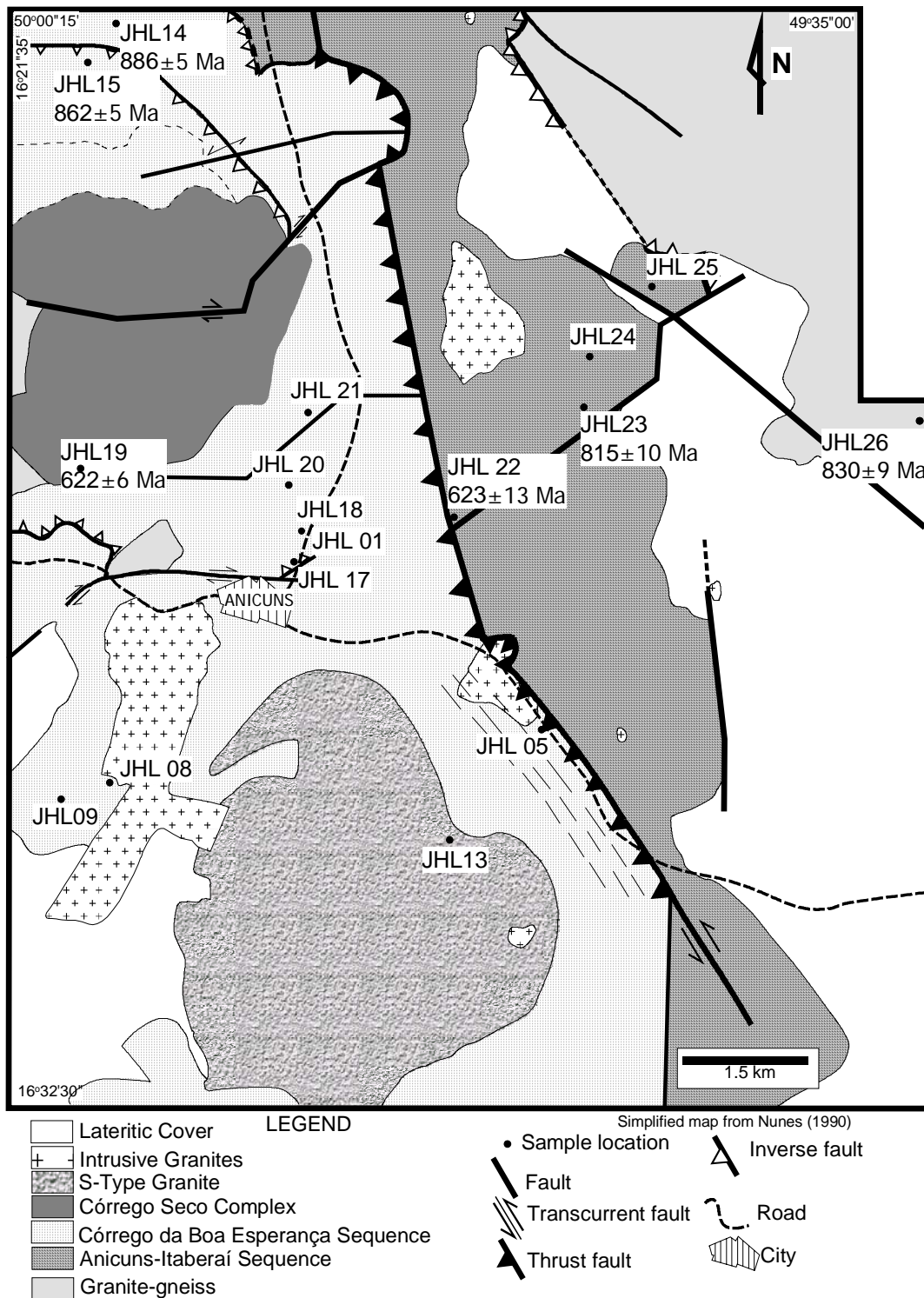


**Figure 4.3** - Geological map of the Anicuns region, with sample location (simplified from Nunes, 1990).



area (Pfrimer et al., 1981; Nilson 1981, 1984; Candia and Girardi, 1985; Winge, 1995). The Americano do Brasil intrusion includes metagabbro, metagabbro-norite, olivine gabbro, amphibolite, metadunite, metaperidotite, metapyroxenite, and hornblendite (Nilson, 1984). The Americano do Brasil complex was emplaced at  $626 \pm 8$  Ma (U-Pb zircon data of Laux et al., 2004a), and the original tholeiitic magma presented positive  $\epsilon_{Nd}(T)$  value of approximately +2.4 (Gioia, 1997) indicating little or no contamination with much older sialic crust. The Serra do Gongomé intrusion has an Rb-Sr isochron age of  $637 \pm 19$  Ma and high initial Sr isotopic ratio (0.7153) indicating interaction with older continental crust (Winge, 1995).

#### 4.4 ANALYTICAL PROCEDURES

Major element analyses were carried out by XRF at the Núcleo de Estudos de Granitos of Universidade Federal de Pernambuco. One aliquot of each sample was placed in an oven at  $1000^{\circ}\text{C}$  for two hours for L.O.I. determination. The samples were fused into small pellets using Li tetraborate at 1:5 proportion. All samples were analyzed in a Phillips XRF spectrometer using an Rh tube, and calibration curves constructed with international reference materials.

REE, Hf, Nb, Zr, Ta, Rb, Sr, Ba, Cs, Th, U, and Pb were analyzed by ICP-MS in the geochemistry laboratories of Memorial University of Newfoundland, Canada. Dissolution was carried out in an HF/HNO<sub>3</sub> mixture in screw top Savillex beakers on a hotplate according to the methodology described by Jenner et al. (1990). Calibration was carried out using the method of standard addition, providing rigorous correction for matrix effects.

Sr, Nd, and Pb isotopic analyses were performed in the Geochronology Laboratory of University of Brasília. Approximately 60 mg of powdered rock samples were dissolved for Sr, Sm, and Nd extraction in successive acid attacks with concentrated HF, HNO<sub>3</sub>, and HCl. Sm, Nd, Sr, and Pb samples were loaded on Re evaporation filaments of double filament assemblies and the isotopic measurements were carried out on a multi-collector Finnigan MAT 262 mass spectrometer in static

mode.

Sm-Nd isotopic analyses followed the method described by Gioia and Pimentel (2000) and were mixed with  $^{149}\text{Sm}$ - $^{150}\text{Nd}$  spike solution and dissolved in Savillex capsules. Sm and Nd extraction of whole-rock samples followed conventional cation exchange techniques, using Teflon columns containing LN-Spec resin (HDEHP – diethylhexil phosphoric acid supported on PTFE powder). Uncertainties of Sm/Nd and  $^{143}\text{Nd}/^{144}\text{Nd}$  ratios are better than  $\pm 0.4\%$  ( $1\sigma$ ) and  $\pm 0.005\%$  ( $1\sigma$ ) respectively, based on repeated analyses of international rock standards BHVO-1 and BCR-1.  $^{143}\text{Nd}/^{144}\text{Nd}$  ratios were normalized to  $^{146}\text{Nd}/^{144}\text{Nd}$  of 0.7219 and the decay constant used was  $6.54 \times 10^{-12} \text{ a}^{-1}$ .  $T_{\text{DM}}$  values were calculated using the DePaolo (1981) model.

Sr was separated from the whole-rock solutions using a conventional ion exchange technique, following Pankhurst and O'Nions (1973). Mass fractionation corrections were made using a  $^{88}\text{Sr}/^{86}\text{Sr}$  ratio value of 8.3752.  $1\sigma$  uncertainty on the measured  $^{87}\text{Sr}/^{86}\text{Sr}$  ratios was better than 0.01%. Sr procedure blanks was less than 300 pg.

For Pb, approximately 50 - 100 mg of powdered rock samples were dissolved in a mixture of 2 mL (40%) HF + 1 mL (65%)  $\text{HNO}_3$  for two days, three days with a mixture of 2 mL (40%) HF + 1 mL (65%)  $\text{HNO}_3$ , and 24 hours in 2 mL 6N HCl. This solution was evaporated and taken in 1 mL 0.6N HBr, and Pb was extracted using columns packed with BioRad X8 anionic exchange resin in 0.6N HBr. Procedures were conducted in clean room conditions and using ultra pure reagents (sub-boiling distillation in Teflon® vials). Most of the samples were treated with the procedure described by Kuritani and Nakamura (2002), with some modifications allowing a more efficient Pb extraction (Gioia, written communication). The chemical procedure for Pb separation consists of one single step. Anionic exchange resin (100  $\mu\text{L}$ ) was packed into a polyethylene column (5 mm high in column with internal diameter of 4 mm). The resin bed was cleaned by flushing the column with 2 mL 6N HCl, followed by 1mL of 0.5N  $\text{HNO}_3$  and 1mL of  $\text{H}_2\text{O}$ . The column was then conditioned with 0.4 mL of 0.6N HBr. 500uL of the sample solution was loaded onto the column and eluted with 3 mL of 0.6N HBr - 0.6N  $\text{HNO}_3$ . Particulate samples were eluted with 3.5mL of the same acid mixture. The lead fraction was extracted with 1 mL of  $\text{H}_2\text{O}$

and dried on a hot plate. Some samples were eluted twice in the column to obtain a cleaner fraction of lead. Mass fractionation was  $< 0,1\%$  for all lead ratios, corrected using NIST 981 standard.

#### 4.5 GEOCHEMICAL RESULTS

Sixteen samples of mafic rocks were analyzed for major, trace and the RE elements (results are in Table 4.1). Samples ANA 19A and ANA 19F correspond to fine-grained amphibolites of the Bonfinópolis Sequence, dated at  $838 \pm 20$  Ma (Piuzana et al., 2003a) (Fig. 4.2) by the SHRIMP U-Pb method. Samples JHL 01, JHL 13, JHL 18 e JHL 09 (Fig. 4.3) are also fine-grained amphibolite samples chemically equivalent to andesites (01, 13 and 18) and metabasalt (09) which are most likely ca. 830 Ma old, based on a reference whole-rock Sm-Nd isochron (Laux et al., 2004a). Samples JHL 14, JHL 15, JHL 22C, JHL 23 and JHL 24 (Fig. 4.3) are coarse-grained amphibolites representing both metadiorites and metagabbros. U-Pb zircon ages of Laux et al. (2004a) are  $886 \pm 5$  Ma and  $623 \pm 13$  Ma, respectively, for samples JHL 14 and JHL 22C, indicating two different events of mafic intrusion. Diorite JHL 19 and quartz diorite JHL 26B are preserved from extensive metamorphic recrystallization and present U-Pb zircon ages of  $622 \pm 6$  Ma and  $830 \pm 9$  Ma, respectively. Chlorite schist JHL 22A and amphibolite JHL 22B, are either metasedimentary rocks or mixed volcanic-sedimentary supracrustal rocks. Sample JHL 29 (Fig. 4.4) is a tonalite.

Major element results of these rocks are not of straightforward interpretation since they represent metavolcanic and metaplutonic rocks dominantly metamorphosed under amphibolite facies during the Neoproterozoic. Despite these limitations, previous studies using major element geochemical data have indicated tholeiitic to calc-alkaline trends and assigned island arc setting for the origin of the original magmas (Nilson, 1981; Barbosa 1987; Nunes, 1990). Although the major element data presented here corroborate this interpretation (Fig. 4.5) we will here concentrate the discussion on trace element results.

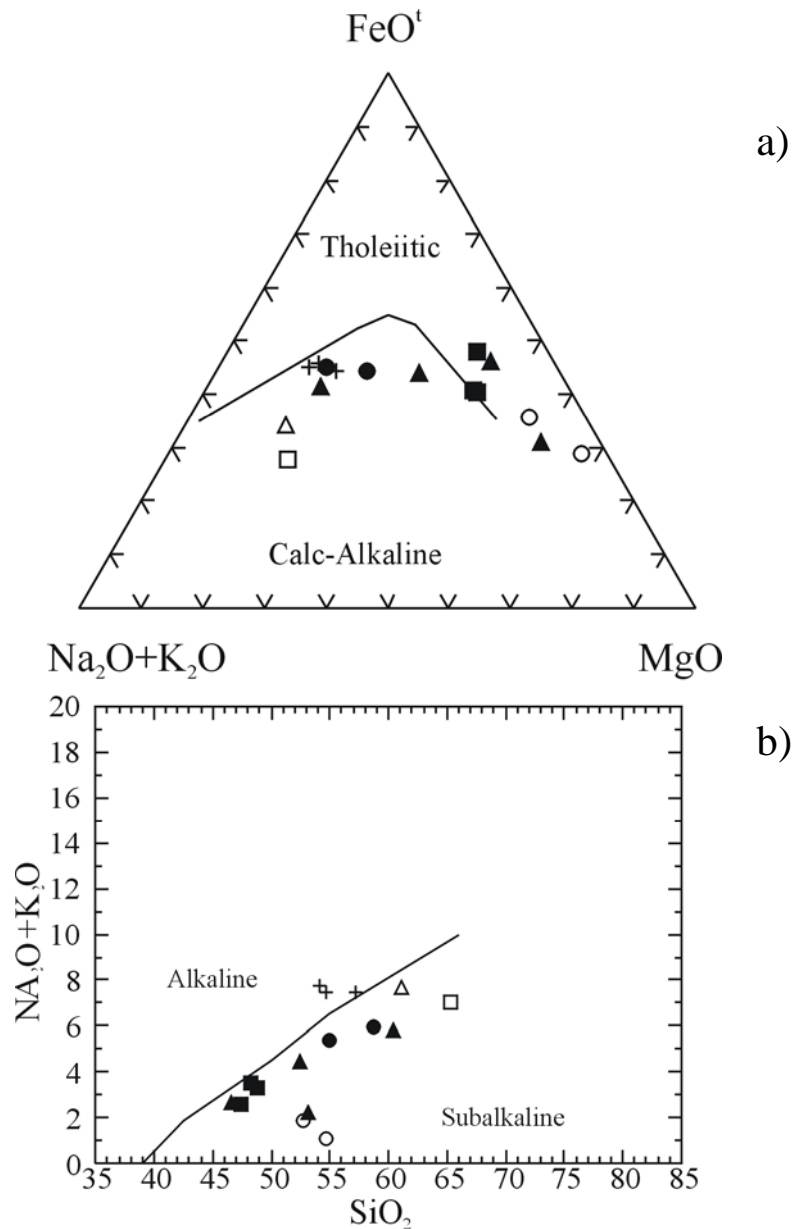


**Figure 4.5** - Tholeiitic/Calc-Alkaline (a) and Alkaline/ Subalkaline (b) diagrams of Irvine and Baragar (1971). Symbols: cross- metandesites, full square- metabasalts, blank square- quartz-diorite, full circle- diorite (ca. 630 Ma), blank circle- metasedimentary rocks, full triangle- diorite (ca.  $\approx$ 830 Ma), blank triangle- tonalite.

Typical trace element patterns of oceanic island arc rocks in multi-element diagrams show LILE (large ion lithophile elements such as Ba, Rb, Cs, Pb, K, U) enrichment and HFSE (High Field Strength Elements) depletion with distinctive troughs in Ti, Zr, Hf, Nb and Ta (Green and Ringwood, 1968; Pearce and Cann, 1973). Two hypotheses have been put forward to explain this pattern (Ringwood, 1990; Foley et al., 2000 and references therein; Churikova et al., 2001). One suggests that HFSE depletion is caused by rutile and/or amphibole, which incorporate

Nb and Ta in their structures and might behave as refractory phases during dehydration or partial melting of oceanic slabs in subduction zones. The second model (e.g. McCulloch and Gamble, 1991) suggests that the Nb and Ta negative anomalies are due to low solubility of these elements in fluids of subduction zones. The amphibolite samples investigated in this study show trace element variation patterns varying from very primitive compositions, similar to N-MORB basalts (Fig. 4.6a), through a group showing moderate LILE enrichment (Fig. 4.6c), to a further group of samples displaying distinctive LILE enrichment (Fig. 4.6b). The N-MORB-like samples are ANA 19A and ANA 19F, which are exposed east of the Anicuns area and are part of the Bonfinópolis Sequence, forming a thrust sheet associated with the Araxá Group metasedimentary rocks. These are most likely representative fragments of Neoproterozoic oceanic floor. All other amphibolite samples have distinctive HFSE depletion. Sample JHL 22A displays an anomalous pattern when compared to the rest, however, this is here interpreted as a metasedimentary rock (Fig 4.6c).

Trace element characteristics of most metabasic rocks investigated are similar to oceanic island arc rocks (Figs. 4.7a and 4.7b), ranging from the tholeiitic to the calc-alkaline series (Figs. 4.7c and 4.7d). REE patterns for these rocks range from those of tholeiitic basalts of MORB to LREE-enriched patterns from island arc basalts (DePaolo and Johnson 1979). A noteworthy feature of all REE patterns is the absence of negative Eu anomalies.

In terms of their REE contents, the samples analyzed may be divided into six groups. The first includes samples with flat chondrite-normalized REE patterns similar to some MORB's (Fig. 4.8a). They also present a small negative Ce anomaly, which has been assigned by some authors as product of interaction with seawater (De Baar et al., 1983; Hole et al., 1984). The second group displays patterns similar to those of calc-alkaline arc andesites with LREE-enrichment and flat HREE pattern (Fig. 4.8a). The third type of REE pattern is the most common in the group of samples investigated representing a steep pattern, with both LREE and HREE fractionation (Fig. 4.8b). The fourth group is formed by metasedimentary rocks which form REE curves which are similar to those of group three, including the absence of negative Eu anomaly (Fig. 4.8c). The fifth group includes samples that display distinctive LREE

fractionation and an upwards-concave HREE pattern (Fig. 4.8d). The sixth pattern is that represented by the tonalite sample, with a very steep curve and slightly concave upward HREE pattern (Fig. 4.8d). Distinctive features of this rock sample is its low Yb content and the relatively high  $(La/Yb)_n$  ratio (approximately 50). This is very similar to REE characteristics of tonalites from other parts of the Goiás Magmatic Arc (Pimentel, 1991, Pimentel et al., 1996) and are also characteristics shared by Archean TTG's and modern adakitic magmas, which are formed by the subduction of young hot oceanic lithosphere (Martin, 1987).

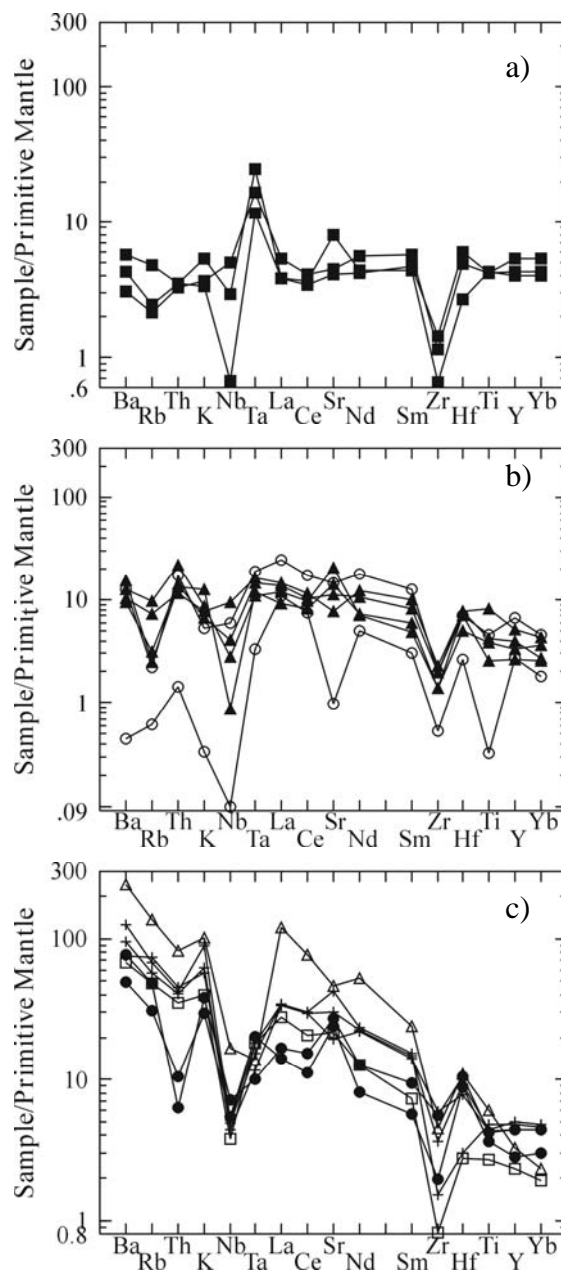


**Figure 4.6** - Spider diagrams normalized to primitive mantle (Sun and McDonough 1989). Symbols are the same from figure 4.5.

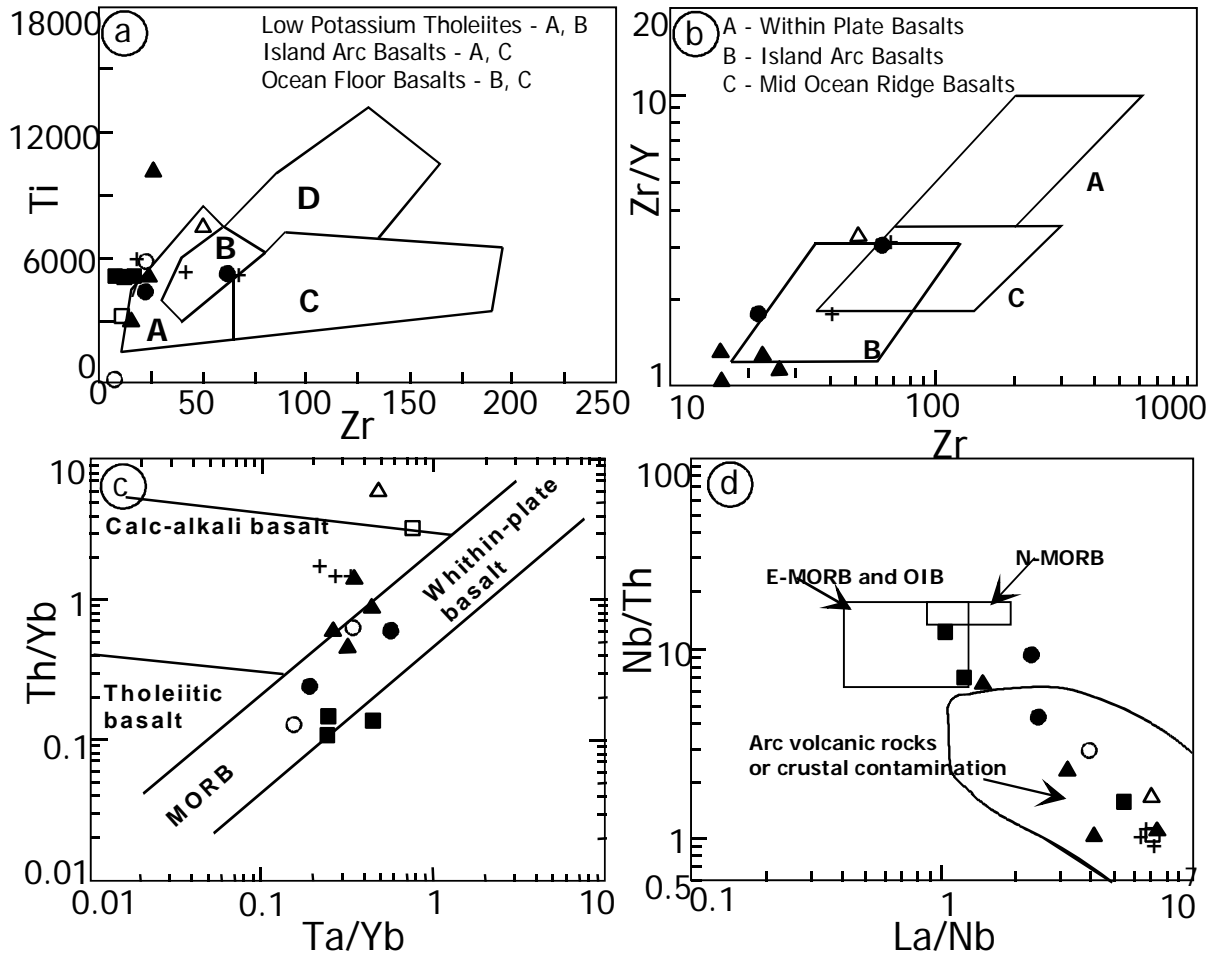


**Figure 4.7** - Tectonic discrimination diagrams, a) Diagram Zr-Ti (Pearce and Cann, 1973); b) Diagram Zr-Zr/Y (Pearce and Cann, 1973); c) Diagram Ta/Yb-Th/Yb (Pearce, 1983); d) Diagram La/Nb-Nb/Th (Pearce, 1983). Symbols are the same from figure 4.5.

#### 4.6 Nd-Sr-Pb ISOTOPES

All rocks analysed present  $T_{DM}$  model ages of ca. 1.0 Ga (Table 4.2), except those of sedimentary origin. This is the typical  $T_{DM}$  pattern of rocks of other parts of the Goiás Magmatic Arc (Pimentel and Fuck, 1992, Pimentel et al., 1996, 1997, Junges et al., 2002).  $\epsilon_{Nd}(T)$  values are positive, indicative of the depleted nature of the mantle source (MORB-like).  $^{147}\text{Sm}/^{144}\text{Nd}$  ratios of most of the mafic rocks investigated are less than 0.19 and indicate a relative enrichment in LREE, which is characteristic of E-MORB or, alternatively, island arc mafic magmas (for more details see Laux et al., 2004a).

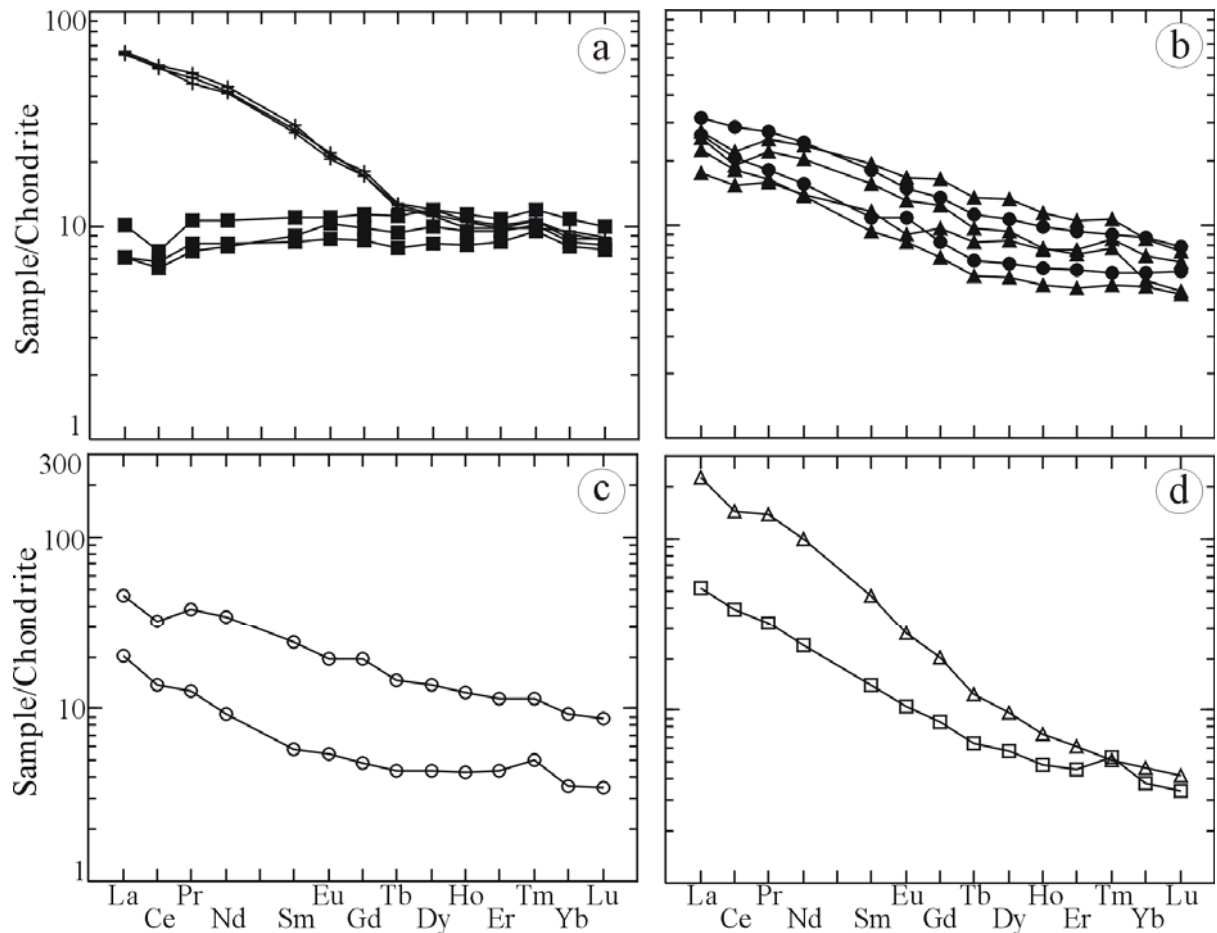


**Figure 4.8** - REE patterns normalized to Chondrite from Taylor and McLennan 1985. Symbols are the same from figure 4.5.

Sr isotopic results (Table 4.3) also indicate the primitive nature of the rocks investigated, with initial  $^{87}\text{Sr}/^{86}\text{Sr}$  ratios between 0.70261 and 0.70335 for the ca. 830 Ma old rocks and between 0.70313 and 0.70557 for the younger group (ca. 630 Ma). Diagram  $\epsilon_{\text{Sr}} \times \epsilon_{\text{Nd}}$  re-calculated for 890 Ma shows that these rocks are not different from those studied by Pimentel and Fuck (1992) in the Arenópolis region, to the west (Fig.4.9).

Pb isotopes display a rather homogeneous composition for the mafic rocks analysed (Table 4.4) and their Pb isotopic ratios are compatible with either arc (orogen) or MORB (mantle) settings (Fig. 4.10).

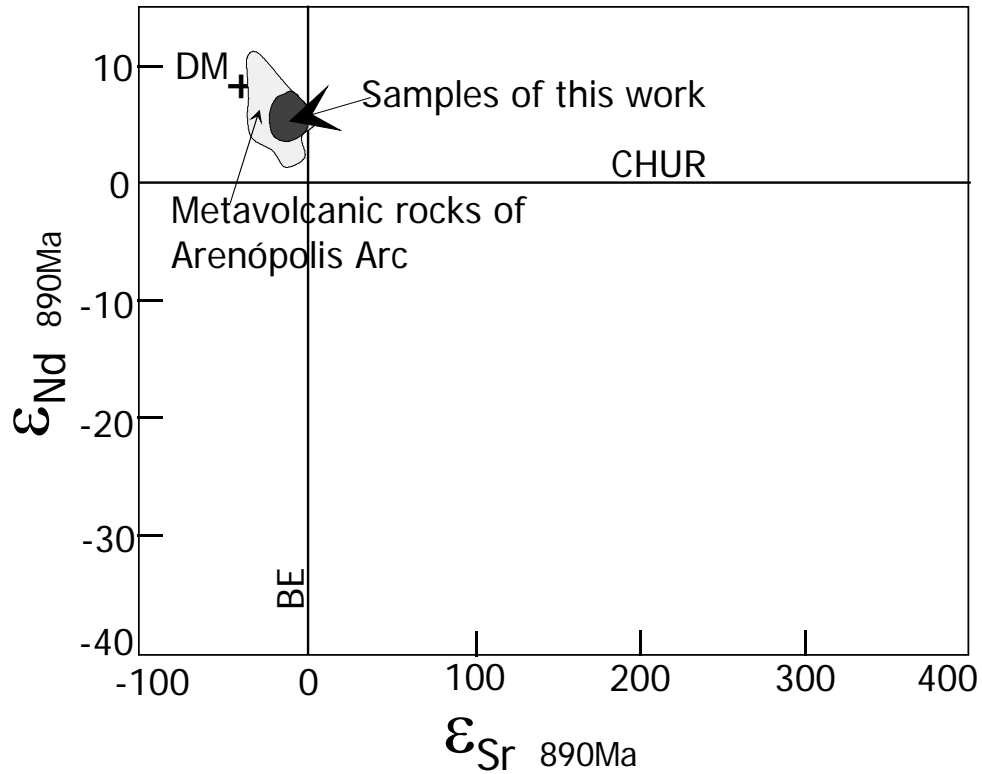


**Figure 4.9** - Plot  $\epsilon_{Sr}$  (T=890Ma) versus  $\epsilon_{Nd}$ (T=890Ma). Field of Arenópolis metavolcanic rocks is from Pimentel (1991).

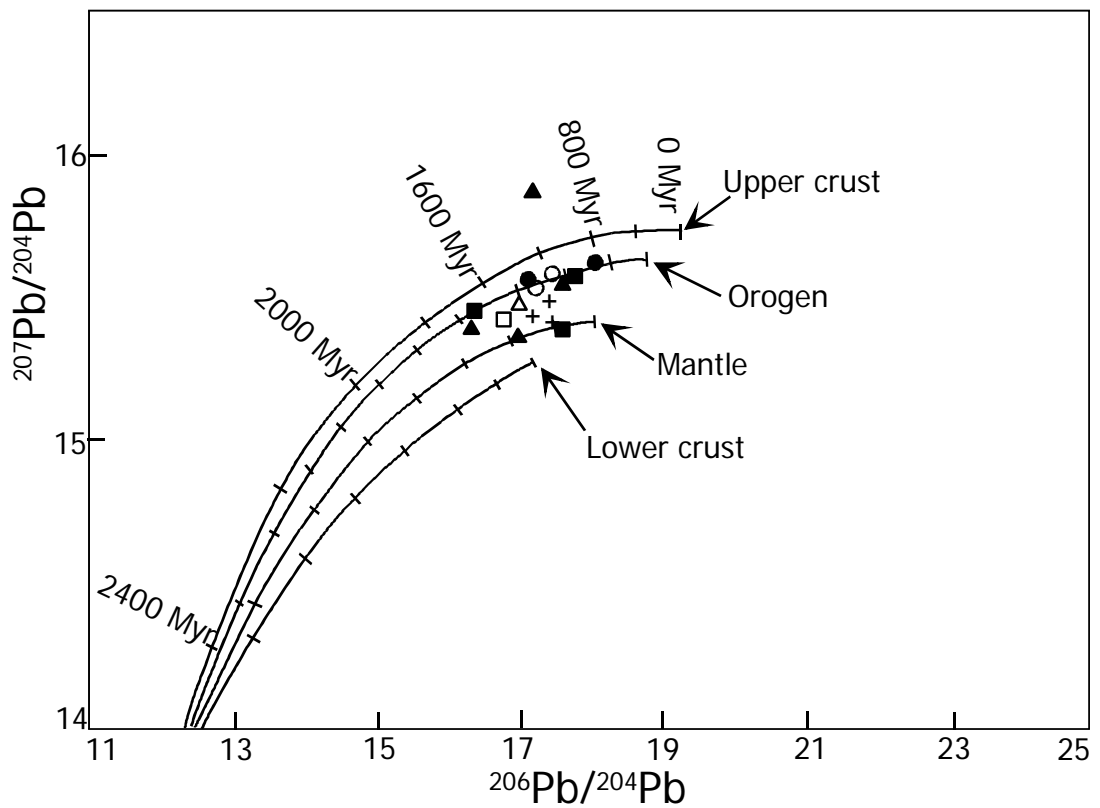


**Figure 4.10** - Pb-Pb isotopic diagram showing isotopic evolution of samples of the area. Reservoirs are from Doe and Zartman (1979). Field of Arenópolis metavolcanic rocks is from Pimentel (1991).

#### 4.7 Nd ISOTOPIC RESULTS OF METASEDIMENTARY ROCKS

Nd isotopic results of sedimentary rocks in the Anicuns area are listed in table 4.5 and displayed in the Nd isotopic evolution diagram of figure 4.11. Sample locations are in figures 4.3 and 4.4.

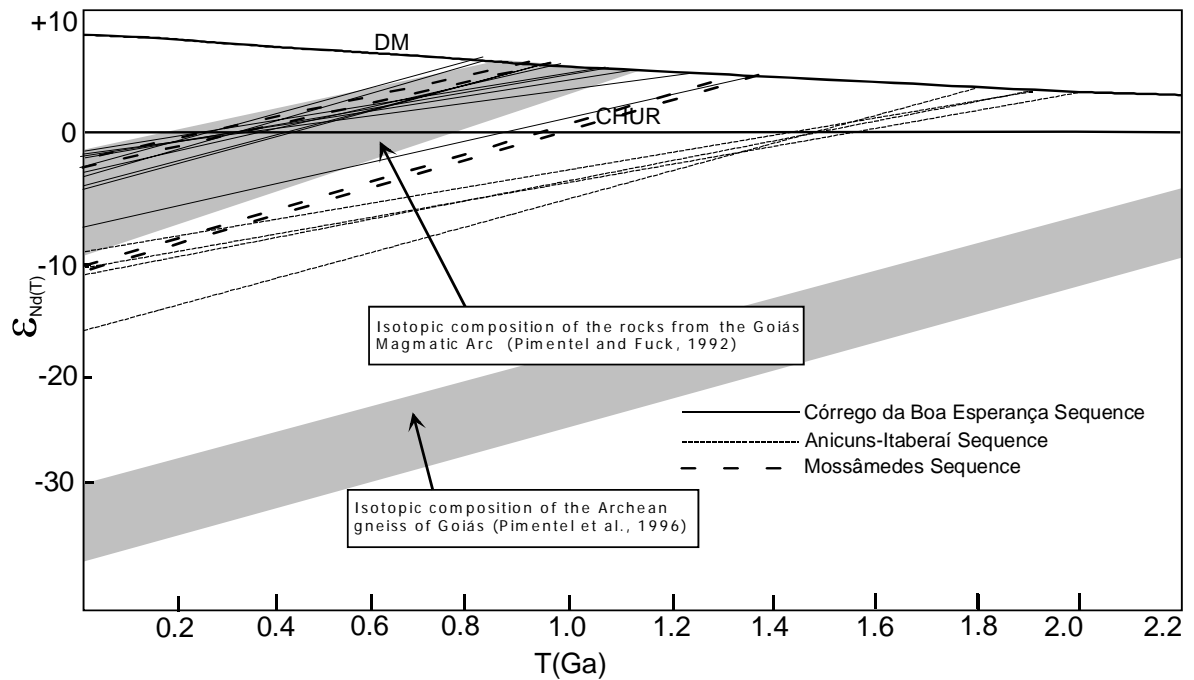


**Figure 4.11** - Evolution  $\epsilon_{Nd}$  x Time diagram showing Nd isotopic composition of the metasedimentary rocks of the Córrego da Boa Esperança, Anicuns-Itaberaí, and Mossâmedes sequences. Nd isotopic composition of the Goiás Magmatic Arc rocks is from Pimentel and Fuck (1992) and of Archean gneisses of Goiás from Pimentel et al. (1996).

Two different groups of Nd isotopic compositions for these rocks can be observed. Rocks belonging to the Anicuns-Itaberaí Sequence have  $T_{DM}$  values between 1.83 and 2.01 Ga, indicating a dominant Paleoproterozoic source region (Table 4.5). On the other hand, samples of the Córrego da Boa Esperança Sequence display  $T_{DM}$  ages between 0.8 and 1.1 Ga, very similar to metagneous rocks of the Goiás Magmatic Arc (Laux et al., 2004a). The original sediments represent, therefore, immature clastic deposits derived from the erosion of the arc itself, without any important contribution from older sources.

Metasedimentary rock samples of the Mossâmedes Sequence are isotopically similar to those of the Córrego da Esperança, although  $T_{DM}$  model ages are slightly older, between ca. 1.0 and 1.4 Ga. The ages show that these rocks are also derived

from the erosion of the juvenile arc with a possible small contribution from an older sialic source.

#### 4.8 CONCLUSIONS

The metamafic samples investigated in this study are tholeiitic to calc-alkaline metabasalts and display major and trace element characteristics that are compatible with an origin within an island arc setting, with LILE enrichment and HFSE depletion. In these settings, LILE enrichment is assigned to metasomatism of the mantle source due to fluids released during slab-dehydration. Amphibolite samples ANA 19A and ANA 19B, of the Bonfinópolis Sequence, associated with sedimentary rocks of the Araxá Group, are slightly different when compared to those of the Anicuns region, and most probably represent fragments of Neoproterozoic ocean floor.

The area of exposure of the Anicuns-Itaberaí Sequence coincides with a regionally important gravimetric discontinuity (Fig. 4.2) suggesting that it marks an important crustal boundary. This is suggested also by the initial isotopic compositions and inheritance patterns (and also initial Sr and Nd isotopic compositions) displayed by the mafic rocks exposed in the Anicuns area. To the west of the gravimetric discontinuity, mafic rocks are pristine, and present positive  $\epsilon_{Nd}(T)$  values, whereas most mafic rock associations towards the east display clear evidence of contamination of the original magmas with older crust. For instance, the Gongomé intrusion has very high initial Sr isotopic ratio (0.7153) (Winge, 1995), rocks of the Santa Bárbara de Goiás Complex have inherited zircon grains of possible Mesoproterozoic age (Laux et al., 2004a), and the Goianira-Trindade layered intrusion has a Sm-Nd isochron age of ca. 621 Ma with an  $\epsilon_{Nd}(T)$  value of 0.0 (M.M. Pimentel, unpublished results).

The Anicuns-Itaberaí and Córrego da Boa Esperança are roughly of the same age (ca. 890 – 830 Ma) (Laux et al., 2004a), however,  $T_{DM}$  values of the sedimentary rocks of these sequences are very distinct from each other. The Córrego da Boa Esperança Sequence sediments, with  $T_{DM}$  values between 0.8 and 1.2 Ga, were

derived mostly from the erosion of the juvenile arc, whereas those of the Anicuns-Itaberaí Sequence indicate derivation from an older, mostly Paleoproterozoic source. In fact, these two sequences are juxtaposed against each other by an important thrust fault zone (Fig. 4.3), suggesting that the original sequences were deposited in different settings, received clastic material from distinct sources, and were later on deformed and tectonically juxtaposed. A similar bimodal behaviour of the provenance pattern of detrital sediments has also been identified in rocks belonging to the Araxá and Ibiá Groups of the Brasília Belt (Fischel et al., 2001a; Pimentel et al., 2001; Piuzeana et al., 2003a). The Anicuns-Itaberaí Sequence may represent a platformal sequence similarly to the model put forward for part of the Araxá basin (for a review see Dardenne, 2000), whereas the Córrego da Boa Esperança Sequence may consist of a near-arc sedimentary basin (arc/fore-arc).

Based on the field, geochronological, isotopic and regional geophysical data, we suggest that the supracrustal sequence exposed in the Anicuns area might represent a arc/fore-arc sequence, marking the tectonic boundary between the Goiás Magmatic Arc and the westernmost exposures of the former São Francisco continental plate.

A likely model for the tectonic setting of this part of the Brasília Belt is illustrated in figure 4.12, in which the Anicuns region might represent the fore arc region of a larger island-arc system.

**Figure 4.12** – Gravimetric anomaly in western Goiás (Baêta Júnior, 1994) compared with the model for island arcs from Gill (1981).

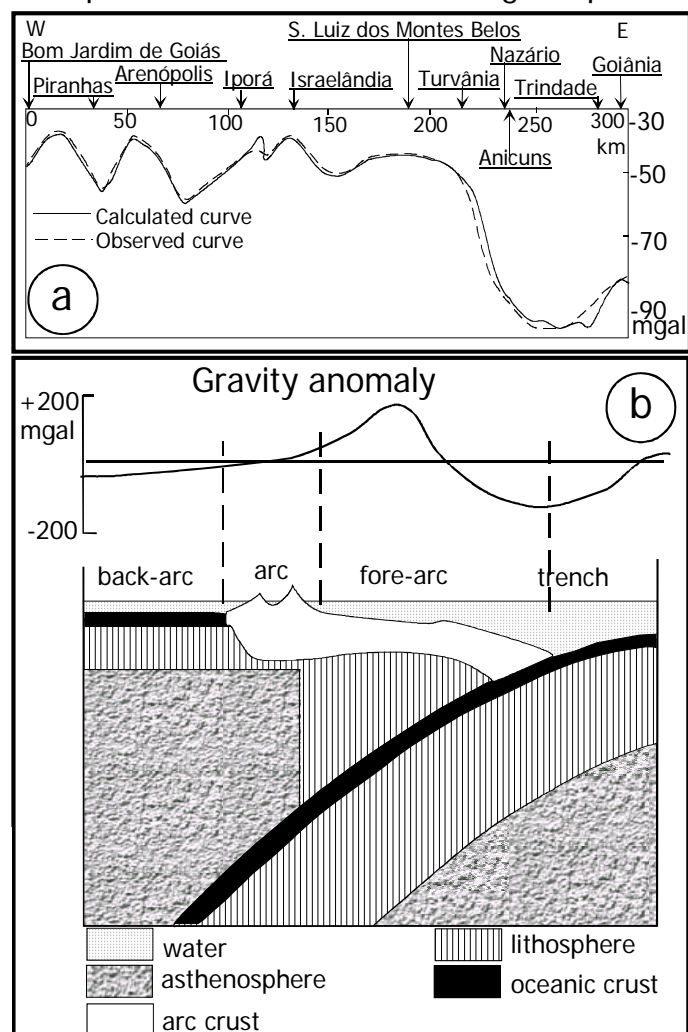


**Table 4.1** - Geochemical results for the samples investigated.

Sample	JHL 01	JHL 09	JHL 13	JHL14	JHL 15	JHL 18	JHL 19	JHL 22A	JHL 22B	JHL 22C	JHL 23	JHL 24	JHL 26B	JHL 29	ANA 19A	ANA 19F
Rock	Amphib. Diorite	Amphib. schist	Quartz Tonalite	Amphib. Diorite	Amphib. Diorite											
Major Elements - X-Ray Fluorecence																
SiO <sub>2</sub> (%)	54.6	47.4	54.1	60.4	52.5	57.2	55.0	54.6	52.1	58.6	53.2	46.6	65.3	61.1	48.8	48.3
Al <sub>2</sub> O <sub>3</sub>	15.0	17.8	15.7	18.2	16.5	14.7	17.7	2.8	9.5	17.9	7.9	10.4	16.2	16.2	15.0	14.5
MgO	3.1	9.1	4.2	2.6	6.5	2.7	4.3	18.9	11.3	2.8	13.9	11.4	2.6	2.6	9.7	9.7
MnO	0.2	0.2	0.2	0.1	0.2	0.2	0.2	0.2	0.1	0.1	0.1	0.2	<0.1	0.1	0.1	0.1
Cão	5.1	9.0	4.4	5.6	8.6	4.9	7.5	11.8	13.5	5.9	13.0	10.9	4.6	3.5	10.4	11.4
Na <sub>2</sub> O	5.6	2.4	5.0	5.6	4.1	5.7	4.5	1.1	1.7	4.8	2.0	2.4	5.8	4.6	3.1	3.4
K <sub>2</sub> O	1.8	0.1	2.7	0.2	0.4	1.7	0.9	<0.1	0.1	1.1	0.2	0.2	1.2	3.1	0.1	0.1
TiO <sub>2</sub>	0.9	0.9	1.0	0.5	0.8	0.9	0.8	<0.1	1.0	0.9	0.9	1.7	0.5	1.3	0.9	0.9
P <sub>2</sub> O <sub>5</sub>	0.8	0.1	0.9	0.1	0.1	0.8	0.2	<0.1	0.2	0.2	0.1	0.1	0.2	0.6	<0.1	0.1
Fe <sub>2</sub> O <sub>3</sub>	9.9	12.1	10.5	6.7	9.6	9.3	8.6	9.1	8.1	8.0	8.0	13.4	4.1	5.9	9.8	10.0
Total	97.3	99.2	99.0	100.2	99.3	98.3	99.7	98.8	98.4	100.6	99.4	97.6	100.7	98.9	98.3	98.6
Trace Elements – ICP-MS																
Li(ppm)	18.1	28.2	27.8	17.3	2.9	22.3	14.8	16.7	10.6	7.8	9.5	10.6	12.6	41.2	12.7	8.7
Rb	36.1	3.1	42.9	6.1	1.6	47.2	19.6	0.4	1.4	30.8	1.9	4.6	30.4	87.0	1.5	1.3
Sr	634.1	166.3	887.9	441.5	296.2	406.1	508.9	20.8	309.6	569.2	239.6	161.5	453.2	968.7	86.5	93.2
Y	22.5	18.0	21.7	11.9	14.9	20.0	12.7	12.2	30.6	20.0	17.8	23.4	10.5	14.6	19.3	24.4
Zr	40.7	7.3	17.1	15.4	15.3	66.0	21.7	5.9	22.3	61.7	22.1	25.4	9.1	50.2	15.9	12.8
Nb	3.5	0.4	3.6	1.9	0.6	3.1	3.9	<0.1	4.2	5.0	2.9	6.8	2.7	11.8	2.0	3.6
Mo	0.3	0.2	0.3	0.1	0.2	0.2	0.3	0.2	0.7	0.4	0.3	0.4	0.2	0.9	0.3	0.2
Cs	1.3	1.1	1.3	0.1	<0.1	1.1	0.7	<0.1	0.1	0.3	0.1	0.2	0.5	3.5	0.1	<0.1
Ba	669.0	40.0	874.0	89.0	106.6	530.3	344.4	3.1	88.7	535.2	66.1	72.7	472.1	1690.6	30.1	21.5
Hf	2.8	0.8	0.9	2.2	1.5	2.4	2.7	0.8	2.2	3.2	2.3	2.3	0.8	3.3	1.8	1.5
Ta	0.6	0.4	0.7	0.4	0.5	0.4	0.8	0.1	0.7	0.4	0.6	0.7	0.7	0.5	1.0	0.6
Pb	9.0	2.3	6.6	9.7	2.9	8.0	4.6	2.2	4.5	4.6	4.8	1.9	4.9	19.7	0.8	0.4
Th	3.5	0.3	3.6	1.8	1.1	3.8	0.9	0.1	1.4	0.5	1.2	0.9	3.0	6.9	0.3	0.3
U	0.9	0.1	0.9	0.4	0.2	0.9	0.3	<0.1	0.7	0.2	0.4	0.2	0.4	1.4	<0.1	<0.1

**Table 4.1** - Geochemical results for the samples investigated (Cont.).

Sample	JHL 01	JHL 09	JHL 13	JHL14	JHL 15	JHL 18	JHL 19	JHL 22A	JHL 22B	JHL 22C	JHL 23	JHL 24	JHL 26B	JHL 29	ANA 19A	ANA 19F
Rock	Amphib. Diorite	Amphib. schist	Amphib. schist	Amphib. schist	Amphib. Quartz	Amphib. Quartz	Amphib. Quartz	Tonalite	Amphib.	Amphib.						
Rare Earth Elements - ICP-MS																
La(ppm)	23.38	2.63	23.78	8.17	6.35	23.27	9.63	7.47	16.82	11.55	9.33	9.96	19.01	81.85	2.60	3.70
Ce	52.30	6.51	53.834	17.22	14.47	52.60	19.77	3.17	31.16	27.33	18.10	20.79	36.88	137.62	6.03	7.24
Pr	6.70	1.14	7.016	2.22	2.14	6.52	2.47	1.71	5.25	3.70	3.02	3.45	4.42	18.85	1.04	1.44
Nd	30.35	5.89	31.442	9.64	9.82	29.58	11.09	6.67	24.48	17.24	14.37	16.66	17.05	70.93	5.71	7.54
Sm	6.53	1.95	6.772	2.14	2.65	6.27	2.50	1.35	5.60	4.14	3.57	4.46	3.21	10.68	2.09	2.51
Eu	1.91	0.75	1.843	0.72	0.78	1.78	0.93	0.48	1.67	1.28	1.11	1.44	0.92	2.43	0.89	0.95
Gd	5.27	2.60	5.513	2.14	2.95	5.22	2.54	1.46	5.89	4.07	3.78	4.96	2.63	6.24	2.99	3.45
Tb	0.72	0.45	0.742	0.33	0.48	0.70	0.39	0.25	0.85	0.64	0.55	0.77	0.37	0.72	0.53	0.64
Dy	4.30	3.14	4.548	2.16	3.21	4.25	2.51	1.67	5.20	4.06	3.51	4.98	2.23	3.72	3.77	4.49
Ho	0.88	0.69	0.907	0.44	0.65	0.82	0.53	0.36	1.04	0.82	0.65	0.95	0.41	0.62	0.80	0.95
Er	2.42	2.08	2.512	1.25	1.91	2.42	1.54	1.09	2.85	2.32	1.79	2.58	1.12	1.54	2.36	2.69
Tm	0.34	0.33	0.379	0.18	0.30	0.37	0.21	0.18	0.40	0.32	0.27	0.37	0.19	0.18	0.36	0.42
Yb	2.34	1.98	2.272	1.26	1.78	2.16	1.47	0.89	2.28	2.14	1.35	2.10	0.94	1.15	2.08	2.65
Lu	0.33	0.29	0.325	0.18	0.25	0.33	0.23	0.13	0.32	0.29	0.18	0.28	0.12	0.16	0.31	0.37

**Table 4.2** Summary of Sm-Nd results for the mafic rocks (after Laux et al., 2004a).

Sample	Sm	Nd	$^{143}\text{Nd}/^{144}\text{Nd}$ ( $\pm 2\text{SE}$ )	$^{147}\text{Sm}/^{144}\text{Nd}$	$\epsilon_{(0)}$	$\epsilon_{(T)}$	$T_{\text{DM}}(\text{Ga})$	$^{143}\text{Nd}/^{144}\text{Nd}_{(T=890)}$
JHL01 <sup>1</sup>	6.16	29.40	0.512517 ( $\pm 05$ )	0.1266	-2.3	--	0.92	0.511778
JHL 09 <sup>1</sup>	2.11	6.42	0.512876 ( $\pm 10$ )	0.1991	4.6	--	--	0.511714
JHL13 <sup>1</sup>	6.60	30.52	0.512524 ( $\pm 17$ )	0.1308	-2.2	--	0.95	0.511760
JHL14 <sup>1</sup>	2.12	9.25	0.512542 ( $\pm 06$ )	0.1387	-1.9	+4.4	1.01	0.511732
JHL15 <sup>1</sup>	2.64	9.95	0.512713 ( $\pm 06$ )	0.1603	1.5	+5.5	0.94	0.511777
JHL18 <sup>1</sup>	6.50	29.23	0.512500 ( $\pm 06$ )	0.1297	-2.7	--	0.98	0.511743
JHL23 <sup>2</sup>	3.44	13.94	0.512612 ( $\pm 06$ )	0.1493	-0.5	+4.4	1.02	0.511740
JHL24 <sup>2</sup>	4.27	15.95	0.512663 ( $\pm 10$ )	0.1620	0.5	--	1.11	0.511717
JHL 26b <sup>2</sup>	3.21	17.01	0.512401 ( $\pm 06$ )	0.1142	-4.6	+4.4	0.98	0.511734
JHL19 <sup>3a</sup>	2.54	10.86	0.512540 ( $\pm 19$ )	0.1412	-1.9	+1.8	1.05	
JHL22a <sup>3b</sup>	1.27	6.29	0.512374 ( $\pm 10$ )	0.1226	-5.1	--	1.11	
JHL22b <sup>3b</sup>	5.28	22.84	0.512538 ( $\pm 05$ )	0.1398	-1.9	--	1.04	
JHL22c <sup>3b</sup>	4.05	16.93	0.512566 ( $\pm 06$ )	0.1447	-1.4	+2.6	1.05	
JHL 29	10.9	72.01	0.512059 ( $\pm 06$ )	0.0915	-11.3		1.22	
ANA 19A	2.02	5.30	0.513103 ( $\pm 04$ )	0.2207	9.1	+6.5	---	0.511815
ANA 19F	2.33	6.78	0.513023 ( $\pm 04$ )	0.2081	7.5	+6.3	--	0.511808

<sup>1</sup>- Córrego da Boa Esperança Sequence; <sup>2</sup>- Anicuns Itaberai Sequence; <sup>3a</sup>- Anicuns-Santa Bárbara Suíte - Córrego Seco Complex (intrusive in Córrego da Boa Esperança Sequence); <sup>3b</sup>- Anicuns-Santa Bárbara Suíte - Córrego Seco Complex (intrusive in Anicuns Itaberai Sequence).

**Table 4.3** Sr isotopic results.

Sample	Rb(ppm)	Sr(ppm)	$^{87}\text{Sr}/^{86}\text{Sr}(\pm 2\text{SE})$	$^{87}\text{Sr}/^{86}\text{Sr}_{\text{Inic.}}$	$\epsilon(\text{T})$	Age(Ga)	$^{87}\text{Sr}/^{86}\text{Sr}_{(\text{T}=0.89)}$
JHL 01	36.13	634.13	0.70496 ( $\pm 2$ )	0.70296	-7.6	0.85	0.70286
JHL 09	3.058	166.29	0.70326 ( $\pm 2$ )	0.70261	-12.5	0.85	0.70258
JHL 13	42.96	887.95	0.70461 ( $\pm 2$ )	0.70291	-8.3	0.85	0.70283
JHL 14	6.10	441.55	0.70397 ( $\pm 2$ )	0.70346	0.1	0.88	0.70346
JHL 15	1.58	296.22	0.70307 ( $\pm 2$ )	0.70288	-8.5	0.86	0.70287
JHL 18	47.24	406.08	0.70648 ( $\pm 2$ )	0.70239	-15.7	0.85	0.70220
JHL 19	19.66	508.91	0.70417 ( $\pm 1$ )	0.70318	-8.3	0.62	----
JHL 22A	0.38	20.88	0.70605 ( $\pm 2$ )	0.70557	25.72	0.63	----
JHL 22B	1.40	309.61	0.70343 ( $\pm 2$ )	0.70331	-6.3	0.63	----
JHL 22C	30.85	569.18	0.70452 ( $\pm 2$ )	0.70313	-9.1	0.62	----
JHL 23	1.96	239.66	0.70363 ( $\pm 2$ )	0.70335	-2.6	0.81	0.70333
JHL 24	4.62	161.52	0.70393 ( $\pm 2$ )	0.70292	-8.1	0.85	0.70288
JHL 26B	30.44	453.21	0.70514 ( $\pm 2$ )	0.70284	-9.7	0.83	0.70267
JHL 29A	87.03	968.74	0.70745 ( $\pm 2$ )	0.70511	19.3	0.63	----
ANA 19A	1.54	86.58	0.70322 ( $\pm 2$ )	0.70261	-12.9	0.84	0.70256
ANA 19F	1.37	93.22	0.70314 ( $\pm 2$ )	0.70263	-12.5	0.84	0.70260

**Table 4.4** Pb isotopic results.

Sample	U (ppm)	Pb (ppm)	Th (ppm)	$^{206}\text{Pb}/^{204}\text{Pb}$	$^{207}\text{Pb}/^{204}\text{Pb}$	$^{208}\text{Pb}/^{204}\text{Pb}$	$^{206}\text{Pb}/^{204}\text{Pb}^*$	$^{207}\text{Pb}/^{204}\text{Pb}^*$	$^{208}\text{Pb}/^{204}\text{Pb}^*$	T(Ga)
JHL 01	0.91	9.03	3.48	18.306	15.572	37.988	16.990	15.484	36.936	0.83
JHL 09	0.10	2.30	0.29	18.110	15.520	37.460	16.818	15.434	37.115	0.83
JHL 13	0.93	6.63	3.61	18.533	15.510	38.102	17.255	15.425	36.611	0.83
JHL 14	0.42	9.74	1.84	17.607	15.475	37.229	16.329	15.390	36.723	0.83
JHL 15	0.23	2.93	1.12	18.174	15.460	37.648	16.921	15.376	36.612	0.83
JHL 18	0.99	8.05	3.85	18.594	15.564	38.564	17.290	15.477	37.242	0.83
JHL 19	0.33	4.65	0.89	18.234	15.572	37.730	17.248	15.512	37.335	0.63
JHL 22A	0.06	2.20	0.12	18.061	15.620	37.737	17.049	15.559	37.625	0.63
JHL 22B	0.70	4.53	1.45	18.472	15.638	37.951	17.463	15.577	37.287	0.63
JHL 22C	0.17	4.62	0.53	18.963	15.702	39.042	17.936	15.640	38.797	0.63
JHL 23	0.39	4.87	1.22	18.668	15.984	38.878	17.108	15.880	38.179	0.83
JHL 24	0.21	1.88	0.99	18.944	15.653	38.462	17.597	15.563	36.996	0.83
JHL 26B	0.45	4.96	3.00	18.003	15.492	38.489	16.725	15.407	36.838	0.83
JHL 29A	1.42	19.76	6.92	18.114	15.488	37.930	17.163	15.430	37.212	0.63
ANA 19A	0.07	0.83	0.29	18.697	15.640	38.731	17.357	15.551	37.751	0.83
ANA 19F	0.07	0.47	0.28	18.795	15.487	38.607	17.538	15.403	36.979	0.83

\* Calculate after a curve of evolution of Pb from Stacey and Kramers (1975) using ISOPLOT version 2.11(Ludwig 2001).

**Table 4.5** Sm-Nd results for the metasedimentary rocks.

Sample	Sm	Nd	$^{143}\text{Nd}/^{144}\text{Nd}$ ( $\pm 2\text{SE}$ )	$^{147}\text{Sm}/^{144}\text{Nd}$	$\epsilon_{(0)}$	$T_{\text{DM}}$ (Ga)
JHL08 <sup>1</sup>	2.79	11.69	0.512557 ( $\pm 18$ )	0.1444	-1.5	1.06
JHL 17 <sup>1</sup>	2.53	10.49	0.512541 ( $\pm 06$ )	0.1461	-1.9	1.12
JHL20 <sup>1</sup>	5.44	21.41	0.512546 ( $\pm 05$ )	0.1535	-1.8	1.24
JHL21 <sup>1</sup>	16.75	98.99	0.512447 ( $\pm 06$ )	0.1023	-3.7	0.82
JHL36A <sup>1</sup>	4.32	14.05	0.512624 ( $\pm 19$ )	0.1857	-0.3	---
JHL36B <sup>1</sup>	6.38	29.69	0.512532 ( $\pm 18$ )	0.1299	-2.1	0.93
JHL37 <sup>1</sup>	9.11	50.14	0.512491 ( $\pm 06$ )	0.1098	-2.8	0.81
JHL38A <sup>1</sup>	3.41	18.02	0.512418 ( $\pm 10$ )	0.1114	-4.3	0.96
JHL38B <sup>1</sup>	4.31	23.72	0.512405 ( $\pm 06$ )	0.1097	-4.5	0.93
JHL 39 <sup>1</sup>	7.01	33.95	0.512491 ( $\pm 07$ )	0.1248	-2.8	0.94
JHL22D <sup>2</sup>	0.45	2.04	0.512027 ( $\pm 24$ )	0.1346	-11.9	1.94
JHL22E <sup>2</sup>	3.38	14.67	0.512054 ( $\pm 11$ )	0.1393	-11.4	2.01
JHL22F <sup>2</sup>	10.42	43.88	0.512133 ( $\pm 04$ )	0.1436	-9.8	1.96
JHL25 <sup>2</sup>	3.61	19.90	0.512789 ( $\pm 06$ )	0.1099	-16.5	1.83
JHL 27A <sup>3</sup>	11.24	66.46	0.512066 ( $\pm 06$ )	0.1022	-11.1	1.32
JHL 28 <sup>3</sup>	2.84	13.87	0.512469 ( $\pm 04$ )	0.1238	-3.3	0.97
JHL 30B <sup>3</sup>	2.54	14.81	0.512043 ( $\pm 06$ )	0.1237	-11.6	1.37
JHL 30D <sup>3</sup>	6.00	25.52	0.512535 ( $\pm 06$ )	0.1420	-2.0	1.07

<sup>1</sup>- Córrego da Boa Esperança Sequence; <sup>2</sup>- Anicuns Itaberaí Sequence; <sup>3</sup>- Mossamedes Sequence).